J|A|C|S
ARTICLES

Published on Web 11/03/2009

Family of Multifunctional Layered-Lanthanum Crystalline Nanowires with Hierarchical Pores: Hydrothermal Synthesis and Applications

Peng-peng Wang,[†,‡] Bo Bai,[†,‡] Shi Hu,[†] Jing Zhuang,[†] and Xun Wang*[,†]

Department of Chemistry, Tsinghua University, Beijing 100084, People's Republic of China, and Department of Chemical Engineering, Institute of Environmental Science and Engineering, Chang'an University, Xi'an 710054, People's Republic of China

Received August 31, 2009; E-mail: wangxun@mail.tsinghua.edu.cn

Abstract: A family of layered-lanthanum crystalline NWs with hierarchical pores was synthesized via a facile hydrothermal route. The diameter of the pores ranged from 2 to 50 nm, covering both the micropore and the mesopore scale. Luminescence was introduced by doping nanowires with Eu^{3+} ion. By combining the merits of hierarchical porous nanowires and layered hydroxides, these as-synthesized products have shown a unique bioengineering application of capturing and releasing short DNA fragments rapidly in dilute solution, and environmental engineering applications due to their remarkable capability to remove organic dye from water.

Introduction

One-dimensional (1D) nanostructures (such as nanowires, nanotubes, nanobelts, and nanorods) have received significant research attention over the past years due to their intriguing properties and promising applications.[1] In particular, porous structures of these 1D nanomaterials have been the focus of recent studies, which further broaden the potential applications in catalysis, bioengineering, environmental protection, sensors, and other areas due to their intrinsic pore structures and high surface-to-volume ratio. Up to now, several methodologies have been developed to achieve these special 1D nanostructures. The thermal CVD method has been used to produce porous GaN nanowires (NWs).[2] Wiley and co-workers reported the synthesis of porous wires from directed assemblies of nanospheres in two porous membranes followed by dissolving of nanospheres.[3] Porous $W_{18}O_{49}$ NWs were also obtained by repeat-filling the colloidal particles in the porous anodic alumina (PAA) template followed by treating at 650 °C.[4] More recently, SiC porous NWs have been achieved via in situ carbonizing Si NWs in 1350 °C,[5] and highly porous CdO NWs were prepared by calcining the hydroxy- and carbonate-containing cadmium compound precursor NWs.[6] However, all of these reported routes either required high post-treatment temperature or involved preparing the materials within a pre-existing template of the desired 1D nanostructures. Moreover, the porous nanostructures prepared by these methods comprise relatively narrow pore distribution and poor crystallinity, which in turn limited their potential application in catalysis, separation, and biological fields. It still remains a great challenge to develop feasible methods for the synthesis of porous 1D nanostructure with hierarchical pore distribution.

Layered double hydroxides (LDHs), with the general formula $[M^{2+}_{1-x}M^{3+}_{x}(OH)_2][(x/n)A^{n-}\cdot mH_2O]$ (M^{2+} and M^{3+} are divalent and trivalent cations, respectively; A represents an anion), are the most extensively studied family of layered hydroxides due to their practical applications in catalysis, separation technology, and biological fields.[7] In general, these LDH materials comprise positively charged layers with anions and water molecules intercalated in the interlayer region, and the interlayer anions can be exchanged for other inorganic or organic anions. In these materials, a family of layered compound containing only one kind of metal cation is called layered hydroxide metal salts

[†] Tsinghua University.
[‡] Chang'an University.

(1) (a) Pan, Z. W.; Dai, Z. R.; Wang, Z. L. *Science* **2001**, *291*, 1947–1949. (b) Peng, Z. A.; Peng, X. G. *J. Am. Chem. Soc.* **2001**, *123*, 1389–1395. (c) Kim, F.; Song, J. H.; Yang, P. D. *J. Am. Chem. Soc.* **2002**, *124*, 14316–14317. (d) Wang, X.; Li, Y. D. *Angew. Chem., Int. Ed.* **2002**, *41*, 4790–4793. (e) Kang, Z. H.; Wang, E. B.; Mao, B. D.; Su, Z. M.; Gao, L.; Lian, S. Y.; Xu, L. *J. Am. Chem. Soc.* **2005**, *127*, 6534–6535. (f) Nakayama, Y.; Pauzauskie, P. J.; Radenovic, A.; Onorato, R. M.; Saykally, R. J.; Liphardt, J.; Yang, P. D. *Nature* **2007**, *447*, 1098–1101. (g) Tian, B. Z.; Zheng, X. L.; Kempa, T. J.; Fang, Y.; Yu, N. F.; Yu, G. H.; Huang, J. L.; Lieber, C. M. *Nature* **2007**, *449*, 885–889. (h) Nah, Y. C.; Ghicov, A.; Kim, D.; Berger, S.; Schmuki, P. *J. Am. Chem. Soc.* **2008**, *130*, 16154–16155. (i) Hochbaum, A. I.; Chen, R. K.; Delgado, R. D.; Liang, W. J.; Garnett, E. C.; Najarian, M.; Majumdar, A.; Yang, P. D. *Nature* **2008**, *451*, 163–167.
(2) Bae, S. Y.; Seo, H. W.; Park, J. H.; Yang, H.; Kim, B. S. *Chem. Phys. Lett.* **2003**, *376*, 445–451.
(3) Li, F.; He, J. B.; Zhou, W. L.; Wiley, J. B. *J. Am. Chem. Soc.* **2003**, *125*, 16166–16167.
(4) Xiao, Z. D.; Zhang, L. D.; Tian, X. K.; Fang, X. H. *Nanotechnology* **2005**, *16*, 2647–2650.
(5) Yang, Y. J.; Meng, G. W.; Liu, X. Y.; Zhang, L. D.; Hu, Z.; He, C. Y.; Hu, Y. M. *J. Phys. Chem. C* **2008**, *112*, 20126–20130.
(6) Guo, Z.; Li, M. Q.; Liu, J. H. *Nanotechnology* **2008**, *19*, 245611.
(7) (a) Fogg, A. M.; Green, V. M.; Harvey, H. G.; O'Hare, D. *Adv. Mater.* **1999**, *11*, 1466–1469. (b) Liu, Z. P.; Ma, R. Z.; Osada, M.; Iyi, N.; Ebina, Y.; Takada, K.; Sasaki, T. *J. Am. Chem. Soc.* **2006**, *128*, 4872–4880. (c) Poul, L.; Jouini, N.; Fievet, F. *Chem. Mater.* **2000**, *12*, 3123–3132. (d) Lee, J. H.; Rhee, S. W.; Jung, D. Y. *J. Am. Chem. Soc.* **2007**, *129*, 3522–3523. (e) Yan, D. P.; Lu, J.; Wei, M.; Han, J. B.; Ma, J.; Li, F.; Evans, D. G.; Duan, X. *Angew. Chem., Int. Ed.* **2009**, *48*, 3073–3076.

(LHSs). To date, a variety of LHSs and their derivatives have been reported, such as $Zn_5(OH)_8(NO_3)_2 \cdot 2H_2O$, $Zn_5(OH)_8(CH_3COO)_2 \cdot 2H_2O$, lanthanide hydroxyhalide materials,[8−10] and so on. Unfortunately, most morphologies of traditional LDHs and LHS are irregular particles, plates, and other shapes;[7b,c,11] few studies have focused on the synthesis of nanowires of LDHs. Such 1D LDHs, which might be assembled in arrays, are attractive building blocks and would be of great importance because of the possible new structural properties induced by their reduced dimensionality.

For rare earth layered hydroxides and their derivatives, they can combine the advantages of lanthanide and layered hydroxides, which is expected to expand the field of layered compounds, endow them with special properties such as luminescence, and make them rather appealing for potential applications such as luminescence, pharmaceutical carriers, and catalysis. Herein, we report a facile hydrothermal approach for the synthesis of porous NWs of layered hydroxide lanthanum acetate (LHL-acetate). Control synthesis was also performed, using formic acid (LHL-formate) or propionic acid (LHL-propionate) instead of acetic acid. The LHL-acetate porous NWs have a diameter of 35 ± 5 nm, and the length reaches to a few micrometers. To the best of our knowledge, this is the first reported synthesis of layered-lanthanum NWs. We further demonstrate that by doping Eu ions into lanthanum layered hydroxide NWs, luminescence can be introduced to the NWs that show typical emission of Eu ions. It is worthy to note that when used in wastewater treatment, the products show remarkable capability to remove organic dye from water. Furthermore, the porous 1D structure and positive charge on the surface make them rather appealing for bioengineering applications in capturing and releasing short DNA fragments rapidly in dilute solution.

Experimental Section

Reagents. Salmon sperm DNA (Sigma No. D-1626) was purchased form Sigma Co. All other reagents used were of analytical grade and were purchased from Beijing Chemical Corp. and used as received.

Synthesis of LHL-Acetate Porous NWs and Eu^{3+}-Doped Samples. In a typical synthesis, $La(NO_3)_3 \cdot 6H_2O$ (0.45 g) was dissolved in a mixture of deionized water (15 mL) and ethanol (10 mL), into which oleylamine (4 mL) was added to form a milky-white suspension, and then acetic acid (0.2 mL) was added drop by drop with vigorous stirring for 15 min. The whole mixture was then sealed in a Teflon-lined autoclave (50 mL capacity). The autoclave was heated and maintained at 160 °C for 12 h and allowed to cool to room temperature. The as-obtained product was collected by centrifugation, and washed with cyclohexane and ethanol, respectively. The NWs were then dried at 60 °C for 4 h. The yield was nearly 100%. Eu^{3+}-doped samples were prepared as described above except for the addition of a proportional amount (1%, 2.5%, 5%, and 10% total molar ratio) of $Eu(NO_3)_3$ to the precursor mixture.

Synthesis of LHL-Formate and -Propionate. The procedure was the same as described above for the synthesis of LHL-acetate, except formic acid (0.13 mL) or propionic acid (0.26 mL) was used instead of acetic acid, respectively.

Shear DNA into Short Fragments. Salmon sperm DNA (3.4 mg) was dissolved in deionized water (10 mL) followed by shaking on the tabletop microtiter shaker at a speed of 7 for 20 min to fully dissolve the DNA, and then the solution was treated using an ultrasonic cell crusher (at 500 W) for 25 s at intervals of 5 s. The resulting solution was stored at 4 °C for use. The size of DNA fragments was determined by gel electrophoresis.

Capture and Release of DNA from Dilute Solution. The particular as-synthesized product (7.5 mg) was added to a solution of DNA fragments (15 mL, 52 μg/mL) under stirring. The flocky precipitates were formed immediately. Next, 0.2 mmol of EDTA-3Na was added to the above mixture. The flocky precipitates disappeared from the solution. The mixture before and after adding EDTA-3Na was centrifuged at 4000 rpm for 5 min, respectively. The two supernatants were used for UV−vis spectra.

Water Treatment Experiment. Ten milligrams of the as-synthesized product was added to 15 mL of Congo red solution (100 mg/L) under stirring. UV−vis absorption spectra were recorded at different intervals to monitor the process.

Characterization. The phase purity of each product was verified by powder X-ray diffraction (XRD) on a Bruker D8 Advance X-ray diffractometer using Cu Kα radiation (λ = 1.5418 Å). The morphologies and structures of the products were observed by using a JSM-6700F scanning electron microscope (SEM) at 10 kV, a JEOL JEM-1200EX transmission electron microscope (TEM) at 120 kV, and a Tecnai G2 F20 S-Twin high-resolution transmission electron microscope (HRTEM) at 200 kV. Nitrogen adsorption/desorption measurements were conducted on a ASAP 2010 V5.02H instrument. TG profiles were collected on Netzsch STA 409 C TGA apparatus from room temperature to 1000 °C, with a heating rate of 20 °C min^{-1} in a nitrogen stream (50 mL min^{-1}). Elemental analysis of C, H, and N was performed using a CE440 elemental analyzer. FTIR spectra were recorded with a Nicolet 205 FTIR spectrometer using the KBr pellet technique. UV−vis absorption spectra were measured on a Hitachi U-3010 spectrophotometer. Fluorescence spectra were recorded using a Hitachi F-4500 fluorescence spectrophotometer.

Results and Discussion

Structure and Morphology. The structure of the products was investigated by powder X-ray diffractometer (XRD). The XRD pattern of LHL-acetate porous NWs (Figure 1a) shows a feature typical of layered structure: sharp reflections in the range of small angles. Interestingly, there are two interlayer spacings of 1.07 and 1.52 nm. The maximum peak at $2\theta = 8.2°$ indicates an interlayer distance of 1.07 nm. The peaks at $2\theta = 16.4°$, 24.6°, and 32.9° can be assigned to the second-, third-, and fourth-order reflections, respectively (marked with *), corresponding to the "1.07 nm phase". Another interlayer spacing is 1.52 nm, showing its corresponding first- and second-order reflections at $2\theta = 5.8°$ and 11.6°, respectively. This structure with two interlayer spacings has been observed for $Yb_2(OH)_5Cl_{1.5} \cdot H_2O$ reported by Poudret et al. and $Zn(OH)_{1.75}(CH_3COO)_{0.26} \cdot 0.57H_2O$ by Song et al.[10] Poudret et al. thought that the presence of two layered phases was due to changes in orientation of the polyhedra within the layer and hence their thickness,[10a] whereas Song et al. proposed that the occurrence of two interlayer spacings resulted from the different orientation of the interlayer water molecules because of the effect of the charged layers and the hydrogen bonding with neighboring hydroxyl groups.[10b] We think the proposal of Song et al. is quite reasonable to accept for the two layer phases in the case of LHL-acetate here, because there is an obvious difference (0.45 nm) between the 1.07/1.52 nm layered phases. For $Yb_2(OH)_5Cl_{1.5} \cdot H_2O$ reported by Poudret et al., the layered phases of 8 and 8.4 Å have a little difference

(8) Morioka, H.; Tagaya, H.; Karasu, M.; Kadokawa, J.; Chiba, K. *Inorg. Chem.* **1999**, *38*, 4211–4216.
(9) Hosono, E.; Fujihara, S.; Kimura, T.; Imai, H. *J. Colloid Interface Sci.* **2004**, *272*, 391–398.
(10) (a) Poudret, L.; Prior, T. J.; McIntyre, L. J.; Fogg, A. M. *Chem. Mater.* **2008**, *20*, 7447–7453. (b) Song, R. Q.; Xu, A. W.; Deng, B.; Li, Q.; Chen, G. Y. *Adv. Funct. Mater.* **2007**, *17*, 296–306.
(11) (a) Oh, J. M.; Hwang, S. H.; Choy, J. H. *Solid State Ionics* **2002**, *151*, 285–291. (b) Hu, G.; O'Hare, D. *J. Am. Chem. Soc.* **2005**, *127*, 17808–17813. (c) Bellezza, F.; Cipiciani, A.; Costantino, U.; Nocchetti, M.; Posati, T. *Eur. J. Inorg. Chem.* **2009**, 2603–2611.

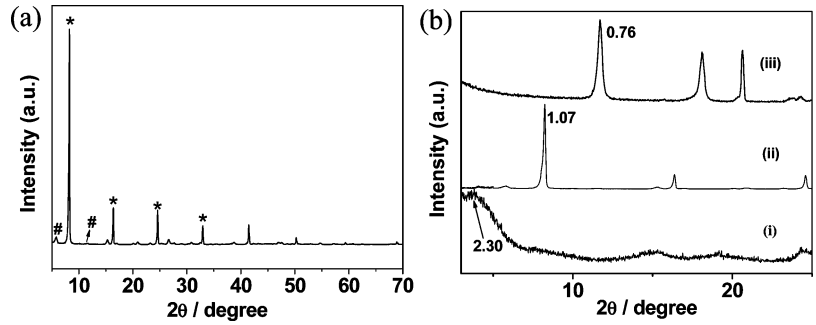

Figure 1. (a) XRD pattern of the LHL-acetate porous NWs showing two interlayer spacings of 1.07 and 1.52 nm; and (b) low-angle XRD patterns of (i) LHL-propionate, (ii) LHL-acetate, and (iii) LHL-formate.

because of slight changes in the layer thickness. The slight changes in the layer thickness, however, could not possibly cause an obvious difference between two layer phases. The sharp peaks in the XRD pattern also suggest that the as-synthesized LHL-acetate porous NWs are highly crystalline. No accurate crystallographic data could be obtained because a single crystal with sizes big enough for crystallographic study could not be gained. However, the structure of LHL-acetate is somewhat analogous to that of $Eu(OH)_{2.5}Cl_{0.5}\cdot 0.8H_2O$ and $[RE_4(OH)_{10}(H_2O)_4]_nA_n$ (RE = rare-earth ions, A = intercalated organic anions, 2,6-naphthalenedisulfonate, and 2,6-anthraquinonedisulfonate).[12] On the basis of the reported structures and our powder XRD and TG results, here we propose that the layered material of LHL-acetate consists of a similar structure: $[La_4(OH)_{10}(H_2O)_4]^{2+}$ cationic layers formed by polyhedra of eight and nine coordinated lanthanum atoms, with the interlayer acetate anions directed toward the cationic layers to compensate for the positive charge. The proposed structure is shown in Figure S1 in the Supporting Information. Figure 1b compares the low-angle XRD patterns of LHL-propionate, -acetate, and -formate. For LHL-formate, the interlayer spacing has decreased from 1.07 to 0.76 nm. By contrast, the interlayer spacing has increased to 2.30 nm for LHL-propionate, although it showed poor crystallinity. The explanation for these changes of interlayer distances is that three different length organic anions came from acids, which have intercalated between hydroxide layers.

The morphologies of the products are examined by scanning electron microscopy (SEM) and transmission electron microscopy (TEM). Figure 2a−f shows the SEM and TEM images of LHL-acetate. The porous nanowires morphology was very pure in the sample, based on TEM characterization. As shown in Figure 2a and b, the LHL-acetate porous NWs have the diameter of 30−40 nm, and the length reaches to a few micrometers. A closer look by SEM indicates that a few NWs assemble parallel to each other (Figure 2a, inset) and thus appear thicker in a low resolution SEM image. Figure 2c and d reveals that these NWs exhibit lots of clearly visible pores throughout the whole length. Careful observation shows that the pores distributed along the axial direction have diameters between 2 and 50 nm, indicating the pore sizes distribution is in the range from micropores to mesopores (Figure 2d). HRTEM analysis and the corresponding FFT pattern (Figure 2e,f) show that the porous NWs are highly crystallized. The pores with broad size distribution and high crystallinity will lead to rough surfaces of the layered hydroxides, which will increase the chemically active sites and contact areas between the nanowires and other species and thus enhance their adsorption or catalysis properties.

The diameter of the LHL-acetate NWs can be controlled by adjustment of the volume ratio of ethanol to water in the hydrothermal conditions. For example, by changing the amount of these two solvents to 15 mL/10 mL, the diameter of NWs can be tuned to ∼16 nm. As a consequence, the diameter of pores decreases with the decrease of NW diameter (Figure 3). The LHL-formate exhibits porous NWs partially similar to that of LHL-acetate (Figure S2 in the Supporting Information and Figure 2g), although the length decreases to 1−2 μm while the diameter increases from 50 to 100 nm. Moreover, the pores distributed along the NWs are somewhat smaller than those of LHL-acetate NWs. By contrast, the LHL-propionate shows morphology of thin NWs without pores (Figure 2h and i), and the diameter of single NW is about 6 nm. We assume that the pores are caused by the inherent layer structures of the compounds. It is well-known that natural/artificial layer structures can form nanotube/nanowires under certain conditions.[13] For layered hydroxides, different interlayer anions will lead to differences in the interaction between layers and anions. In our study, it is most probable that the layer compound has a tendency to form nanotubes; however, the interaction between interlayer anions and layers causes the collapse beginning from defects and then extending to pore structures. In the case of LHL-propionate, the smaller diameters of the NWs restrict the extension of collapse, and thereby no porous structures formed. In addition, oleylamine gives a pH of about 9.5 to the reaction system, which provides the basic surrounding for the formation of layered hydroxide; meanwhile, it plays an important role to guide the anistropic growth of one-dimensional nanowires in the synthesis, and on the basis of our experimental results only $La(OH)_3$ nanorods can be obtained if NaOH were used to replace oleylamine. Dodecylamine can also play the same role at the hydrothermal temperature of 180 °C (Figure S3 in the Supporting Information).

NWs Compositions and Characterizations. In general, LHL derivatives show different stoichiometry in the composition rations of metal, hydroxyl group, organic anions, and water molecules. To estimate the chemical formula of obtained products, elemental analysis and thermogravimetric analysis (TGA) are used. The chemical formula can be expressed as $La(OH)_{1.99}(CH_3COO)_{1.02}\cdot 0.61H_2O$, $La(OH)_{2.06}(HCOO)_{0.94}\cdot$

(12) (a) Geng, F. X.; Xin, H.; Matsushita, Y.; Ma, R. Z.; Tanaka, M.; Izumi, F.; Iyi, N.; Sasaki, T. *Chem.—Eur. J.* **2008**, *14*, 9255–9260. (b) Gandara, F.; Perles, J.; Snejko, N.; Iglesias, M.; Gomez-Lor, B.; Gutierrez-Puebla, E.; Monge, M. A. *Angew. Chem., Int. Ed.* **2006**, *45*, 7998–8001.

(13) (a) Wang, X.; Li, Y. D. *Inorg. Chem.* **2006**, *45*, 7522–7534. (b) Hu, S.; Wang, X. *J. Am. Chem. Soc.* **2008**, *130*, 8126–8127. (c) Wang, X.; Sun, X. M.; Yu, D. P.; Zou, B. S.; Li, Y. D. *Adv. Mater.* **2003**, *15*, 1442–1445. (d) Wang, X.; Li, Y. D. *Chem.—Eur. J.* **2003**, *9*, 5627–5635.

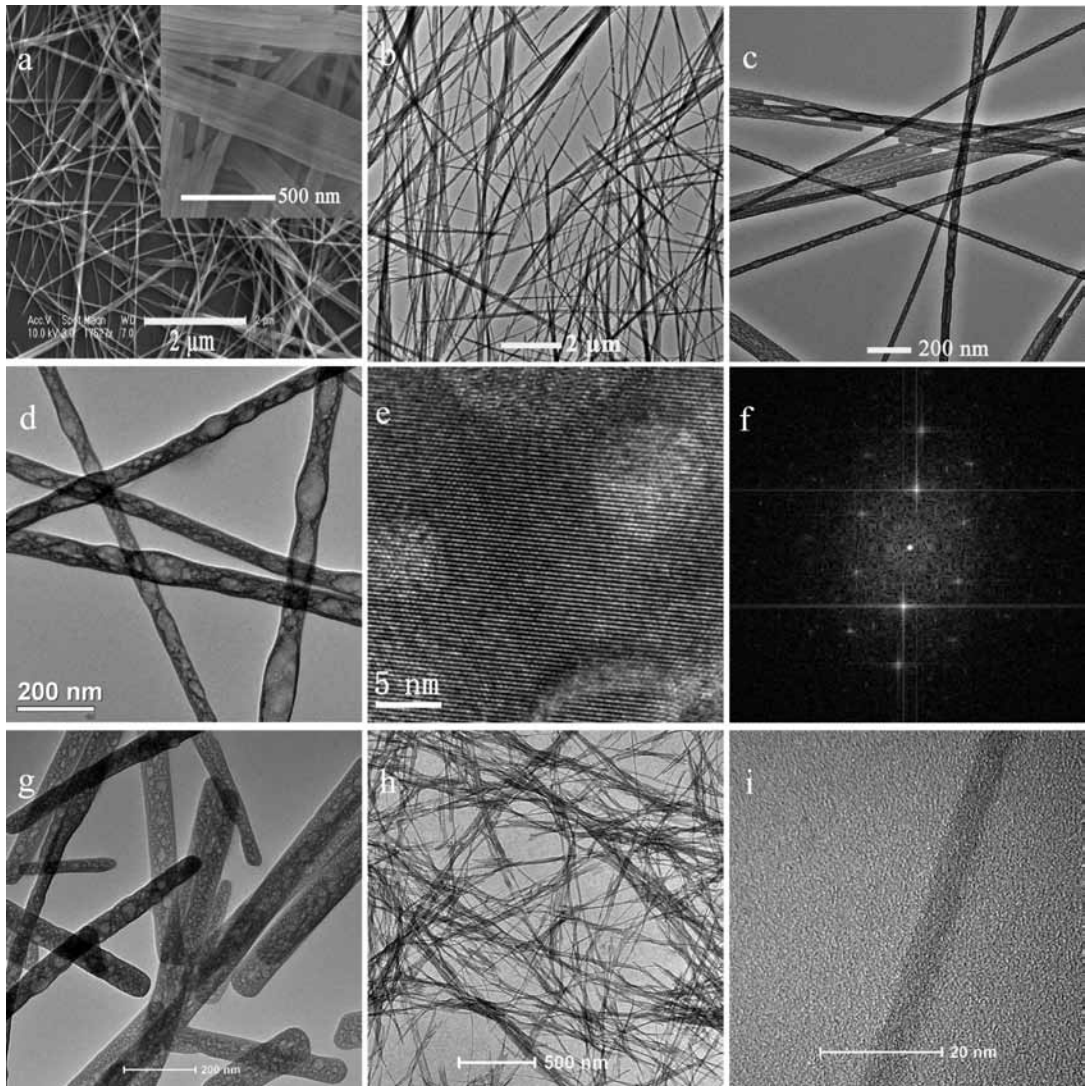

Figure 2. (a) SEM image of LHL-acetate porous NWs (the inset shows a blow-up SEM image of the NWs, indicating the aggregation of some NWs into bundles); (b−d) TEM images of the LHL-acetate porous NWs in different magnification; (e) HRTEM image of an individual LHL-acetate porous NW; (f) FFT pattern of (e); (g) TEM image of LHL-formate NWs; and (h,i) TEM images of LHL-propionate thin NWs.

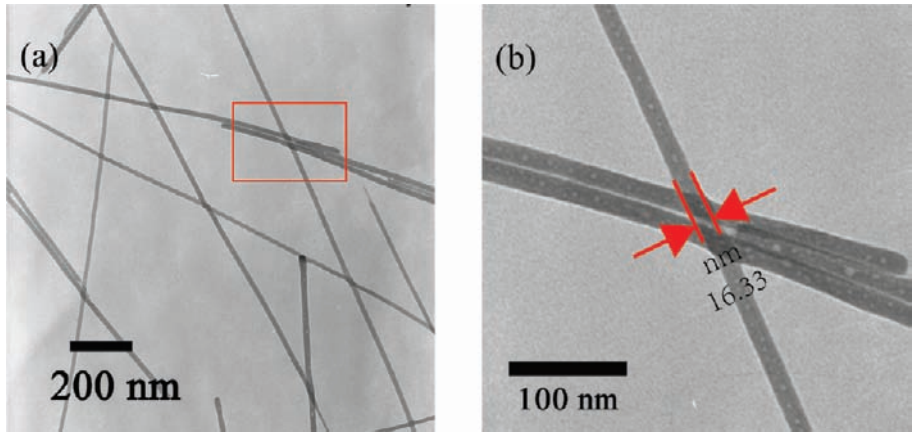

Figure 3. (a) TEM image of LHL-acetate porous NWs with diameter ~16 nm. (b) A partly enlarged image of (a).

$0.22H_2O$, and $La(OH)_{2.28}(C_2H_5COO)_{0.72}\cdot 0.55H_2O$ (see the Supporting Information, Table S1).

The TG curve for $La(OH)_{1.99}(CH_3COO)_{1.02}\cdot 0.61H_2O$ is given in Figure 4a, which is similar to that reported previously for hydroxide nitrate and organo derivatives.[14] In the curve, four stages of mass loss are observed. The first stage shows a mass loss of 4.5% below 200 °C corresponding to the removal of the interlayer water. The second and third stages correspond to dehydroxylation of the hydroxide layers and decomposition of acetate, respectively. The fourth stage by 730 °C results from

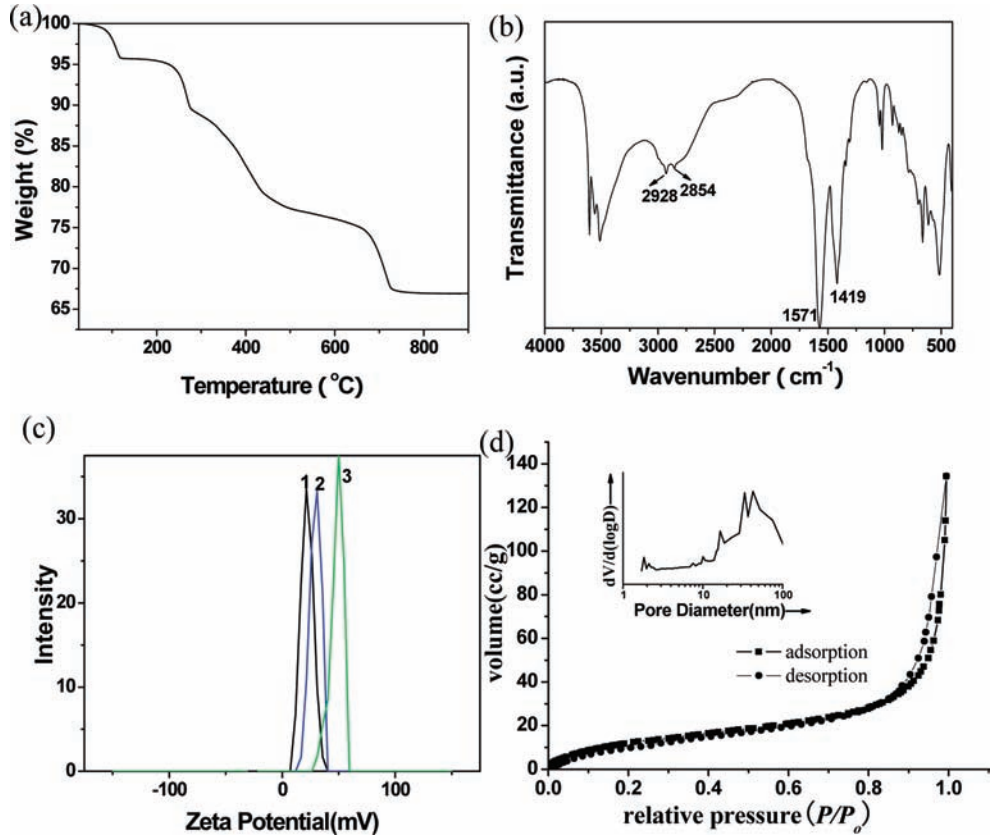

Figure 4. (a) TG curve for $La(OH)_{1.99}(CH_3COO)_{1.02}\cdot 0.61H_2O$ porous NWs showing four stages. (b) FTIR spectrum of the LHL-acetate porous NWs. (c) Zeta potential of (1) LHL-acetate porous NWs, (2) LHL-formate, and (3) LHL-propionate thin NWs directly dispersed in water, respectively (pH = 7.96, concentration: 0.06 mg/mL). (d) N_2 adsorption adsorption/desorption isotherm of LHL-acetate porous NWs. The inset shows the pore size distribution curve obtained from the desorption data.

the decomposition of $La_2O_3CO_3$.[14b] No significant change can be observed above this temperature, and XRD of the residual product reveals it to be La_2O_3 (Figure S4 in the Supporting Information). The TG curve show a total mass loss of about 33%. TG curve for LHL-formate shows the mass loss of 1.8% (4.1% for LHL-propionate) for the interlayer water and total mass loss of 26% (32% for LHL-propionate), as seen in Figure S5 in the Supporting Information.

Further characterization of the LHL-acetate is carried out by Fourier transform infrared spectroscopy (FTIR). As shown in Figure 4b, bands observed in the range 3400−3600 cm^{-1} are due to hydroxyl groups and water, and two bands at 2928 and 2854 cm^{-1} correspond to C−H stretching vibration. The strong bands centered at 1571 and 1419 cm^{-1} are assigned to the symmetric and asymmetric COO^- stretches, respectively, of the acetate groups of the intercalated acetate anions. These bands were also observed in other layered hydroxide metal carboxylate systems.[7c,15] FTIR analyses confirm partially the presence of acetate, hydroxide groups, and water in the LHL-acetate.

To investigate the surface charge of the products in water, the amount of as-prepared samples was directly dispersed in deionized water to form a homogeneous solution. The zeta potential of the products is approximately 22.4 mV for LHL-acetate, 31.4 mV for LHL-formate, and 47.0 mV for LHL-propionate, respectively (Figure 4c), which indicates that the surface of the products is positively charged.

The pore structures and surface area of two porous samples have been further confirmed through Brunauer−Emmett−Teller (BET) analysis. N_2 adsorption/desorption isotherms and corresponding Barrett−Joyner−Halenda (BJH) pore size distribution plots for two porous NWs are shown in Figure 4d and Figure S6. The isotherms show type IV isotherms with a distinct hysteresis loop at partial pressures >0.85, which indicates the presence of textural mesopores.[16] This characteristic signature of textural mesoporosity is observed all over the two NWs. The specific surface areas for LHL-acetate and -formate porous NWs estimated from the BET method are 56.7 and 20.23 $m^2\ g^{-1}$, respectively. These values are expected to be superior to that of the same dimensional NWs, which is generally attributed to the high porosity. The size of the pores based on desorption data exhibits a wide distribution for LHL-acetate samples centered at 2, 10, 16, 33, and 44 nm (Figure 4d, inset), and a distribution for LHL-formate samples centered at 3, 30, and 45 nm (Figure S6 in the Supporting Information), covering the range of both mesopores and macropores, which are consistent with TEM images.

Luminescence can be introduced by doping the LHL-acetate with different Ln^{3+}. XRD patterns of Eu^{3+}-doped samples show that the samples at low doping concentrations keep the main peaks of LHL-acetate; however, when the doping concentration increases to 10%, the structure changed to some extent, and the relative intensity between the peak at 6° and 8° changed significantly (Figure S7 in the Supporting Information). The diameter of NWs decreases to some extent, and a few spheres can be observed after the doping process. Figure 5 shows the photoluminescence spectra of LHL-acetate:Eu NWs with different doping concentrations. The Eu^{3+}-doped samples primarily exhibit luminescence in the range of 580−700 nm, which correspond to transitions from the excited $^5D_0$ level to the ^7F_J

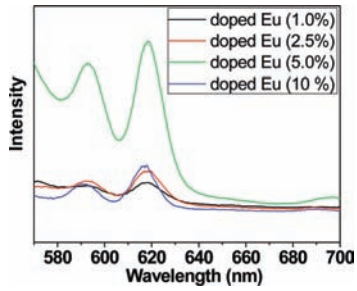

Figure 5. Photoluminescence spectra of LHL-acetate:Eu NWs ($\lambda_{exc} = 268$ nm).

($J = 1, 2, 3, 4$) levels.[17] The strong peaks at 592 and 618 nm are attributed to the $^5D_0-^7F_1$ and $^5D_0-^7F_2$ transitions, respectively. It is worth noting that the sample with doping concentration 5.0 mol % Eu^{3+} displays the highest emission. Further increasing the doping concentration to 10% will decrease the emission intensity. This quenching of the luminescence at high Eu^{3+} doping concentration is often observed when the distance between neighboring europium ions decreases below a critical value, which can generally be attributed to the possible nonradiative transfer resulted from resonance energy transfer between neighboring lanthanide ions.[18]

Capture and Release of Short DNA Fragments in Dilute Solution. As we know, double-stranded DNA is a helical molecule and highly negatively charged. The as-synthesized NWs show high specific surface areas and positive charges on the surface, which inspire us to explore the possible application in separating and recovering DNA in dilute solution. Separation and purification of DNA are of vital significance in bioscience and biotechnology. Silica powder has been widely used for separation of DNA, which adsorbed DNA on their surface. However, it is not suitable for DNA less than 500 bp. Capture of such short DNA in solution and recovering them rapidly at the proper time are still challenges to overcome.[19] Considering this point, we decided to use as-synthesized products for the separation of short DNA fragments.

The separate abilities of NWs for short DNA fragments were evaluated by means of UV−vis absorption spectra. First, to get relatively short DNA fragments, Salmon sperm DNA solution was treated under ultrasonic treatment for 25 s. The sizes of DNA fragments were determined by electrophoresis. A smear of DNA (Figure 6a, lane 1) down the lane represents large pieces of DNA that were sheared into thousands of smaller fragments, and the sizes of DNA fragments were in the range from 300−1400 bp according to the DNA size marker.

When the LHL-acetate porous NWs (7.5 mg) mixed with the solution of above short DNA fragments (15 mL, 52 μg/mL), white flocky precipitate was formed immediately (Figure 6b, inset). The supernatant centrifuged at 4000 rpm for 5 min was used for UV−vis absorption. As shown in Figure 6b, the supernatant of DNA solution shows an absorption maximum at approximately 260 nm (curve 1), which can be attributed to the typical ultraviolet absorption peak of nucleic acids. In contrast, after LHL-acetate porous NWs were added into DNA solution, the supernatant lost the peak at this position (curve 2). This indicates that the DNA fragments have been adsorbed by porous NWs and subsequently removed with NWs by centrifugation. When an amount of EDTA-3Na is added into the mixture of NWs and DNA solution, the peak is almost recovered, indicating most DNA fragments have been recovered. It is also confirmed that the flocky precipitate disappears after adding 0.2 mmol of EDTA-3Na in the solution. We consider that excessive EDTA has coordinated metal ions to form a stable complex, which consumes all of the metal ions of the porous NWs; thus the captured DNA could be released into the solution.

For LHL-propionate thin NWs and -formate porous NWs, the capabilities of DNA separation were also investigated (Figure S8 in the Supporting Information). After EDTA-3Na was added into the mixture of LHL-propionate thin NWs and DNA solution, the peak at 260 nm was recovered at about one-half of its intensity, indicating that DNA captured by LHL-propionate thin NWs were not released completely. One possibility is that the NWs have thin diameter and large BET surface (146.33 $m^2\ g^{-1}$). This characteristic leads to the closer connection with DNA fragments, which make it hard to separate them from each other. However, LHL-formate porous NWs show ineffective ability for DNA separation (Figure S8b in the Supporting Information).

Zeta potential of the products indicates the synthesized products are positively charged on the surface. This characteristic may make the NWs adsorb DNA, due to electrostatic interactions with the negatively charged phosphate groups on the DNA backbone. However, an LDH with a positive surface charge shows ineffective ability of DNA separation (Figure S9 in the Supporting Information). This indicates that the capability of DNA separation by LHL-acetate porous NWs is not only because of electrostatic attraction. Since both DNA and as-synthesized NWs are one-dimensional structures, they may "bond" to each other properly. The lengths of DNA fragments are 100−470 nm, as estimated from the size (300−1400 bp) and the distance between two base pairs (0.34 nm). The width of double-strand DNA is about 2 nm. These two dimensions are much larger in the case of synthesized NWs. It would be possible for DNA chains to entwine around the NWs, as seen in the DNA complex where DNA wrapped around the dendronized polymer.[20] For shorter DNA fragments, they tend to be adsorbed on the surface of NWs. On the basis of this wide pore structure, high specific surface areas, the comparison of two dimensions of DNA and NWs, and a significant fact that DNA can be absorbed on the NWs surface by electrostatic attraction, it is concluded that the DNA chains may entwine around the positively charged, wide porous NWs, as illustrated in Figure 6c and d. For a shorter DNA fragment, it is too short to entwine around the NWs; therefore, a few short DNA fragments may be adsorbed on the NWs.

Wastewater Treatment. Water pollution has become very serious; it can be harmful to people's health and is ultimately setting the limits on human development. Considerable efforts have been made to solve this problem in recent years. Now it

(14) (a) Gobichon, A. E.; Auffredic, J. P.; Louer, D. *Solid State Ionics* **1997**, *93*, 51–64. (b) Newman, S. P.; Jones, W. *J. Solid State Chem.* **1999**, *148*, 26–40.
(15) McIntyre, L. J.; Jackson, L. K.; Fogg, A. M. *Chem. Mater.* **2008**, *20*, 335–340.
(16) Pauly, T. R.; Liu, Y.; Pinnavaia, T. J.; Billinge, S. J. L.; Rieker, T. P. *J. Am. Chem. Soc.* **1999**, *121*, 8835–8842.
(17) (a) Wegh, R. T.; Donker, H.; Oskam, K. D.; Meijerink, A. *Science* **1999**, *283*, 663. (b) Yan, R. X.; Li, Y. D. *Adv. Funct. Mater.* **2005**, *15*, 763–770.
(18) (a) Li, Z. H.; Zeng, J. H.; Zhang, G. C.; Li, Y. D. *J. Solid State Chem.* **2005**, *178*, 3624–3630. (b) Pi, D. B.; Wang, F.; Fan, X. P.; Wang, M. Q.; Zhang, Y. *Spectrochim. Acta, Part A* **2005**, *61*, 2455–2459.
(19) Ichinose, I.; Huang, J. G.; Luo, Y. H. *Nano Lett.* **2005**, *5*, 97–100.
(20) Gssl, I.; Shu, L. J.; Schlter, A. D.; Rabe, J. P. *J. Am. Chem. Soc.* **2002**, *124*, 6860–6865.

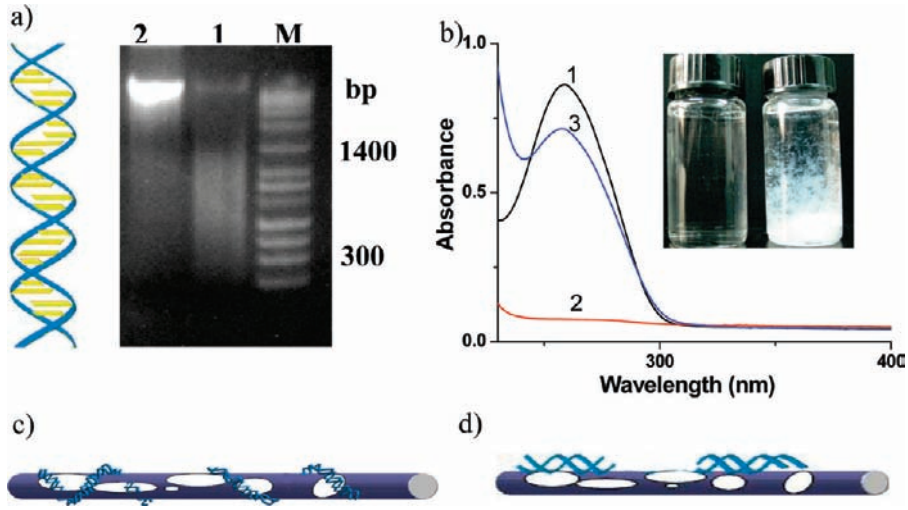

Figure 6. (a) Double-stranded DNA model and DNA electrophoresis patterns (lane 1 is for DNA fragments, lane 2 is for raw DNA); (b) UV−vis absorption spectra of aqueous solutions of salmon sperm DNA. (1) Black curve, DNA; (2) red curve, DNA + LHL-acetate porous NWs; (3) blue curve, DNA + LHL-acetate porous NWs + EDTA; inset of (b) shows aqueous solution of salmon sperm DNA (left) and flocky precipitates of DNA + LHL-acetate porous NWs (right). All of the spectra are determined using supernatant separated from the corresponding solution by centrifugation at 4000 rpm for 5 min. Concentrations of DNA and EDTA are 52 μg/mL and 13.3 mM, respectively; (c and d) schematic illustrations of the binding modes of DNA fragments on porous NWs.

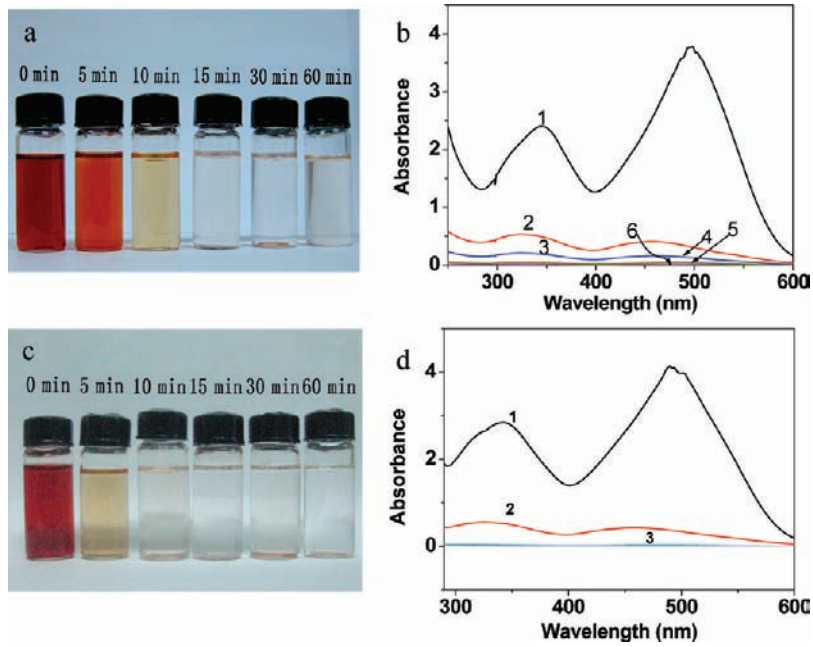

Figure 7. (a) Photo image of absorption of Congo red by LHL-acetate porous NWs at different times; (b) absorption spectra of a solution of Congo red (100 mg/L, 15 mL) in the presence of LHL-acetate porous NWs (0.01 g) at different time intervals: (1) 0; (2) 5; (3) 10; (4) 15; (5) 30; (6) 60 min, respectively; (c) photo image of absorption of Congo red by LHL-propionate thin NWs at different times; and (d) absorption spectra of a solution of Congo red (100 mg/L, 15 mL) in the presence of LHL-propionate thin NWs (0.01 g) at different time intervals (curves 4, 5, and 6 overlap with each other).

has been proved that nanomaterials can be used to remove organic pollutants and toxic ions from water, and these materials show higher removal capacities than do their bulk counterparts.[21] Considering their porous structures or high BET surface area, we proposed that as-synthesized NWs would be quite effective in removing organic pollutants.

Herein, three different products as-synthesized using different acids are used to investigate the application in wastewater treatment. Congo red, a common azo-dye in the textile industry, is chosen as a typical organic pollutant. When the initial concentration of Congo red in water solution is 100 mg/L, both the as-synthesized LHL-acetate porous NWs and the LHL-propionate could nearly remove 100% of the Congo red at room temperature, as confirmed by the photo images and UV−vis absorption spectra at different times in Figure 7. We should note that above 15 min, the color of Congo red remained unchanged (this time is 10 min for that of LHL-propionate), indicating all of the Congo red in the solution should be removed by NWs within 15 or 10 min. This result coincided with UV−vis absorption (curves 4, 5, and 6 in Figure 7b and d overlap with

(21) (a) Zhang, G. S.; Qu, J. H.; Liu, H. J.; Cooper, A. T.; Wu, R. C. *Chemosphere* **2007**, *68*, 1058–1066. (b) Zhong, L. S.; Hu, J. S.; Liang, H. P.; Cao, A. M.; Song, W. G.; Wan, L. J. *Adv. Mater.* **2006**, *18*, 2426–2431.

each other closely). The total adsorption capacities for Congo red were estimated to be 270 and 470 mg/g for LHL-acetate porous NWs and LHL-propionate NWs (Figure S10 in the Supporting Information). This excellent dye removal ability may be partially attributed to electrostatic attraction between NWs and Congo red. Meanwhile, wide porous structures or high BET surface (56.7 $m^2 g^{-1}$ for LHL-acetate and 146.33 $m^2 g^{-1}$ for LHL-propionate) will lead to rough surfaces of the layered hydroxides, which will increase the contact areas between NWs and thus enhance their adsorption performance. However, as-synthesized LHL-formate shows poor ability for removal of Congo red (Figure S11 in the Supporting Information). This may be caused by relatively low BET surface (20.23 $m^2 g^{-1}$). As compared to the commercial activated carbon (Figure S12 in the Supporting Information), the as-synthesized materials have the advantages of rapid adsorption and high removal capacity for Congo red, which will find application in printing and dyeing industries.

Conclusion

In summary, on the basis of a facile hydrothermal route, we have for the first time synthesized LHL-acetate multifunctional porous NWs with hierarchical pore distribution, high crystallinity, and large BET surface. Luminescence property could be introduced by doping other ions. An excellent separation technique for short double-stranded DNA has also been demonstrated here. Meanwhile, the as-synthesized NWs show rapid removal ability for an organic pollutant in wastewater. We believe that these porous NWs are expected to expand the field of layered compounds and result in a further wide application in bioengineering, environmental, and catalytic fields.

Acknowledgment. This work was supported by the NSFC (20725102, 50772056), the Foundation for the Author of National Excellent Doctoral Dissertation of People's Republic of China, the Program for New Century Excellent Talents of the Chinese Ministry of Education, the Fok Ying Tung Education Foundation (111012), and the State Key Project of Fundamental Research for Nanoscience and Nanotechnology (2006CB932301).

Supporting Information Available: Proposed structure of LHL-acetate, TEM images of LHL-acetate NWs synthesized in dodecylamine, chemical results of products, XRD patterns of Eu^{3+}-doped samples and the residual product obtained after the TG measurement, characterization of LHL-formate and -propionate (TEM and TG), the parallel experiment in which DNA was separated by an LDH, and adsorption experiments for Congo red. This material is available free of charge via the Internet at http://pubs.acs.org.

JA907043B